



1 **Shell hash promotes growth in Pacific littleneck clams (*Leukoma*** 2 ***staminea*) by altering pore water chemistry**

3 Hannah L. Kempf^{1,2}, Alyssa J. Griffin^{1,2}, Tessa M. Hill^{1,2}, Tsim D. Schneider³, Sandra J. Carlson^{1*}, David
4 A. Gold^{1,2*}

5 ¹Department of Earth and Planetary Sciences, University of California Davis, Davis, CA 95616, USA

6 ²Bodega Marine Laboratory, University of California Davis, Bodega Bay, CA 94923, USA

7 ³Department of Anthropology, University of California Santa Cruz, Santa Cruz, CA 95064, USA

8 *These authors contributed equally to this work.

9
10 Correspondence to: David A. Gold (dagold@ucdavis.edu)

11 **Abstract.** Bivalves that build calcium carbonate skeletons are at particular risk from ocean acidification, and mitigation
12 strategies will be needed to keep coastal populations healthy. It can be energetically costly for organisms like clams and
13 mussels to build their shells under low pH conditions, and acidification can lead to shell dissolution. Adding crushed shells
14 (shell hash) to beach sediments, a practice used by some Indigenous communities and aquaculturists, may mitigate the negative
15 effects of ocean acidification by altering the chemistry of the pore fluids they live in. We tested the hypothesis that mixing
16 shell hash into the sediment improves the growth and physiology of infaunal Pacific littleneck clams (*Leukoma staminea*).
17 Juvenile clams (pre-sexual maturity) were raised for 90 days under four conditions: control seawater with sediment, acidified
18 seawater with sediment, control seawater with sediment plus shell hash, and acidified seawater with sediment plus shell hash.
19 Pore water and overlying seawater were sampled three times a week for pH, alkalinity, salinity, temperature, and dissolved
20 oxygen. Clam shell weight, soft tissue weight, and new shell growth were measured, and mantle tissue RNA was collected for
21 gene sequencing after three months. Our results demonstrate that the addition of shell hash increased the pH of porewater
22 relative to the control, and animals exposed to acidified water plus shell hash grew larger than animals exposed to acidified
23 water alone. Gene expression profiling suggests that animals in acidified seawater with shell hash were largely
24 indistinguishable from animals in non-acidified water. Our experimental results suggest that adding shell hash to sediments
25 alters the chemistry of pore fluids, thus buffering against acidic conditions that can negatively affect the growth of
26 economically and culturally important shellfish like littleneck clams.



27 **1 Introduction**

28 Anthropogenic carbon dioxide (CO₂) inputs are disrupting the natural acid buffering feedbacks of the Earth system— leading
29 to a ~30% increase in ocean acidity globally since pre-industrial times (e.g., Zeebe and Wolf-Gladrow, 2001; Caldeira &
30 Wickett, 2003; Sabine et al. 2004; Zachos et al., 2008; Doney et al., 2009; Hönisch et al., 2012). As the ocean absorbs excess
31 anthropogenic CO₂, it also shifts carbonate system equilibria towards lower concentrations of carbonate ions, an important
32 building block for calcium carbonate shells/skeletons (Caldeira and Wickett, 2003; Kleypas et al. 1999; Orr et al., 2005). Ocean
33 acidification therefore makes it energetically costly for calcifying marine invertebrates, including animals like corals and
34 shellfish, to build their shells and skeletons, and acidic conditions can dissolve these structures (e.g., Kleypas et al. 1999; Green
35 et al., 2004, 2009; Orr et al., 2005; Waldbusser et al., 2015; Bednaršek, 2019). Given the threats ocean acidification poses to
36 global ecosystems, mitigation strategies are of growing interest to scientists, managers, and the public (e.g., Curtin et al., 2022;
37 Mackenzie et al., 2022; Macreadie et al., 2019; Renforth & Henderson, 2017; Saderne et al., 2019).

38
39 Despite the concern, the impact of ocean acidification on particular species can be hard to predict, particularly on infauna—
40 animals that live within the sediment and are not directly exposed to overlying waters (Ries et al., 2009; Andersson and
41 Mackenzie, 2011; Widdicombe et al., 2011; Dodd et al., 2021; Gold & Vermeij, 2023). This is in part because of the complexity
42 of carbonate chemistry in pore water (i.e. water within the sediment grains), which is clearly related to the overlying seawater
43 chemistry but is generally lower in pH (Widdicombe et al., 2011). Processes that impact pore water pH include microbially-
44 mediated redox reactions, abiotic mineral precipitation/dissolution, and mixing of sediments by macrofauna (Burdige et al.,
45 2008; Dashfield et al., 2008; Kindeberg et al., 2020; Widdicombe et al., 2011). On the one hand, these naturally low pH
46 environments may suggest infaunal bivalves are well-adapted to deal with ocean acidification (Gold and Vermeij 2023).
47 Alternatively, if shellfish fail to cope with the rapid pace of anthropogenic climate change, coastal ecosystems, commercial
48 aquaculture, and communities dependent on shellfish for food security will suffer (e.g., Doney et al., 2020).

49
50 Attempts have been made to mitigate the effects of ocean acidification on bivalves. In the early 2000s, Pacific Northwest
51 commercial oyster hatcheries experienced widespread collapse associated with coastal acidification (Feely et al., 2012; Barton
52 et al., 2015). In response, hatchery, government and academic scientists began to explore methods to buffer seawater used in
53 shellfish culture. For example, this included adding soda ash (Na₂CO₃) to seawater in larval rearing tanks (Barton et al., 2015;
54 Clements & Chopin, 2017; C. L. Mackenzie et al., 2022). In the northeastern United States, adding pulverized shell hash to
55 mudflats was shown to increase the pH of sediment pore waters, and increase settlement of the clam *Mya arenaria* (Green et
56 al., 2009, 2013). Similarly, Ericson and Ragg (2021), demonstrated that rearing tanks enriched with mussel (*Perna canaliculus*)
57 shell hash enhanced *P. canaliculus* larval shell development under high pCO₂ conditions. Despite these promising studies,
58 others have found little to no effect of shell hash on sediment chemistry or infauna. It therefore remains unclear how/if chemical
59 buffering of acidification will improve growth and survival under future ocean acidification scenarios, and may depend on



60 what species is of interest, their habitat preferences, and regional oceanography (Greiner et al., 2018; Beal et al., 2020; Doyle
61 & Bendell, 2022). Controlled experimental studies of the impacts of shell hash and acidification on growth, physiology, and
62 survival of infaunal clams of the same age and genetic stock are needed to help disentangle these variables.

63
64 There is also significant evidence from traditional ecological knowledge that shell hash could be beneficial to bivalve health.
65 Adding shell material back into intertidal sediments and/or creating spaces where shell hash naturally accumulates is one
66 component of complex Indigenous mariculture systems (Lepofsky et al., 2015; Tadlock, 2019; Toniello et al., 2019),
67 particularly along the Northwest coast of North America. Indigenous “clam gardens” promote healthy coastal ecosystems and
68 provide food security (Deur et al., 2015; Groesbeck et al., 2014; Jackley et al., 2016; Lepofsky et al., 2015; Toniello et al.,
69 2019). Although exact management techniques vary by location, clam gardening often involves the purposeful addition of
70 pulverized shell material, or “shell hash,” into beach sediments (Deur et al., 2015; Greiner et al., 2018; Groesbeck et al., 2014;
71 Salter 2018). The existing published research on clam gardens demonstrates that they host larger populations of clams and
72 greater intertidal biodiversity (Groesbeck et al. 2014; Toniello et al., 2019; Cox et al., 2019; Jackley et al., 2016).

73
74 For this study, we examine the impacts of acidification and shell hash addition on infaunal Pacific littleneck clam (*Leukoma*
75 *staminea*) calcification and genetics. All individuals were collected from the Bodega Bay region in Northern California. *L.*
76 *staminea* is an excellent focal species, as it is geographically widespread, relatively abundant, and ecologically and culturally
77 significant (Fraser and Smith, 1928; Lepofsky et al., 2015; Schneider et al., 2018). It is a marine venerid bivalve that burrows
78 5-15 cm beneath the sediment surface along nearly the entire coast of western North America, ranging from Baja California,
79 Mexico to Alaska (Fraser & Smith, 1928). Found in wide-ranging habitats, including exposed rocky beaches and low-energy
80 mudflats, *L. staminea* have been managed and harvested, along with other clam species, by Indigenous peoples across the
81 northeastern Pacific coast for millennia (Lepofsky et al., 2015; Schneider et al., 2018; Toniello et al., 2019) and remain
82 commonly collected and eaten by humans today. It is also an important food source within intertidal food webs, and is preyed
83 upon by drilling gastropods, sea stars, crabs, birds, and sea otters (Feder et al., 1979; Hiebert, 2015). Like many bivalves, *L.*
84 *staminea* is a suspension feeder, metabolizing ambient water that they take in with their siphons, while living in an infaunal
85 environment where pore fluids affect their development once shell formation commences (Fraser and Smith, 1928). *L.*
86 *staminea* grows a shell composed of the calcium carbonate polymorph aragonite, and contains light and dark banding patterns
87 in the outer shell layers (Fraser & Smith, 1928; Takesue and van Geen, 2004; Kempf et al., 2023). The shells’ banding patterns
88 correspond with geochemical and microstructural changes in the shell, and significant size variability can exist within
89 populations of the same age (Kempf et al., 2023). Recent research has documented *L. staminea* population decline in some
90 parts of the British Columbia coast, perhaps due to competition with invasive species (Bendell, 2014). Additional research
91 suggests that some *L. staminea* populations have declined at least partly in response to oceanographic changes in salinity and
92 temperature (Barber et al., 2019), but information regarding the specific impacts of acidification on *L. staminea*, particularly



93 in juveniles, is lacking in the current literature. We hypothesized that shell hash would increase the pH, total alkalinity and
94 saturation state with respect to aragonite (Ω_{Ar}) of pore fluids, resulting in enhanced calcification and a loss of pH-stress genetic
95 signatures in juvenile *L. staminea* exposed to experimental acidification.

96 **2 Materials and Methods**

97 **2.1 Broodstock collection and husbandry**

98 Juvenile clams used in this study were sampled from a single genetic cohort from a controlled spawn in the lab, with parent
99 individuals collected live from Bodega Harbor in Bodega Bay, CA (Kempf et al., 2023). Bodega Bay is located approximately
100 60 miles north of San Francisco on the coast of California, and sits within the California Current System (CCS) where seasonal
101 upwelling creates large natural fluctuations in pH (Hickey & Banas, 2003; Feely et al., 2008; Checkley & Barth, 2009; Davis
102 et al., 2018; Largier, 2020).

103
104 Adult broodstock *L. staminea* collected from Bodega Harbor during the winter of 2021 (n = 22) were brought to the UC Davis
105 Bodega Marine Laboratory (BML) in Bodega Bay, CA for conditioning. Seawater is supplied to the laboratory via intake lines
106 approximately 200 ft offshore. Intake elevation is approximately six feet below mean low tide, and water is sand-filtered to
107 ~30 μ m before being gravity-fed to the facilities. Broodstock were placed in an open plastic basket (10" x 6") and set within a
108 water table filled with circulating seawater. During the 6-week conditioning period clams were fed twice a day with a dense
109 mixture of *Nannochloropsis oculata* and *Isochrysis spp.* algae. These species were chosen by BML aquaculturists as their
110 preferred diet for raising juvenile bivalves. During the first week, seawater temperature gradually increased ~1°C/day from
111 11°C to 17°C to condition the clams for spawning. The system was maintained with a steady influx of filtered seawater, and
112 waste was siphoned from the holding containers daily. To check if clams were gravid, two animals were chosen, and the
113 visceral mass was gently scraped with a scalpel. The gonadal fluid from these clams was pipetted onto a microscope slide and
114 mixed with a small amount of seawater and checked for the presence of eggs or sperm.

115
116 Once gravid, all conditioned clams (n=20) were rinsed with ~20°C seawater and placed in clean baskets inside a 10-gallon
117 container. The seawater was then slowly heated to ~24°C using a heated stirring rod. After reaching this temperature, 30 L of
118 dense *N. oculata* was added, and clams fed for one hour while adjusting to room temperature (~18 °C). Two additional feedings
119 of algae heated to 30°C followed at one-hour intervals. Each time the clams fed for a total of 2 hours in darkness. As spawning
120 had still not occurred, one clam was opened, sperm was confirmed, and gonadal fluid was pipetted into the setup to induce
121 spawning. After two more hours at ~24 °C, clams were fed a final time with 10 L of *N. oculata* and *Isochrysis*, then left
122 overnight as the system gradually cooled to room temperature (~20 °C). By morning, the remaining 19 clams had spawned.

123



124 Planktonic larvae were removed from the spawning container the following morning with a siphon, and transported into 400
125 L tanks in the Bodega Marine Laboratory Shellfish Hatchery. Once larvae began to settle at the bottom of the tank (three weeks
126 post-fertilization), they were transferred onto a 250 micron settling screen and placed in a shallow water table supplied with
127 filtered seawater in the same hatchery room (18-20 °C). Lights were kept on during the day and turned off at night, and salinity
128 was maintained between 33-36 ppt and checked approximately every 3 days. The entire cohort was fed twice weekly with a
129 30 L mixture of *N. oculata* and *Isochrysis* algae. All individuals were kept in identical laboratory conditions during the juvenile
130 rearing period (200 days). At 200 days old, juveniles were transported to the experimental conditions outlined below.

131 2.2 Experimental design and treatments

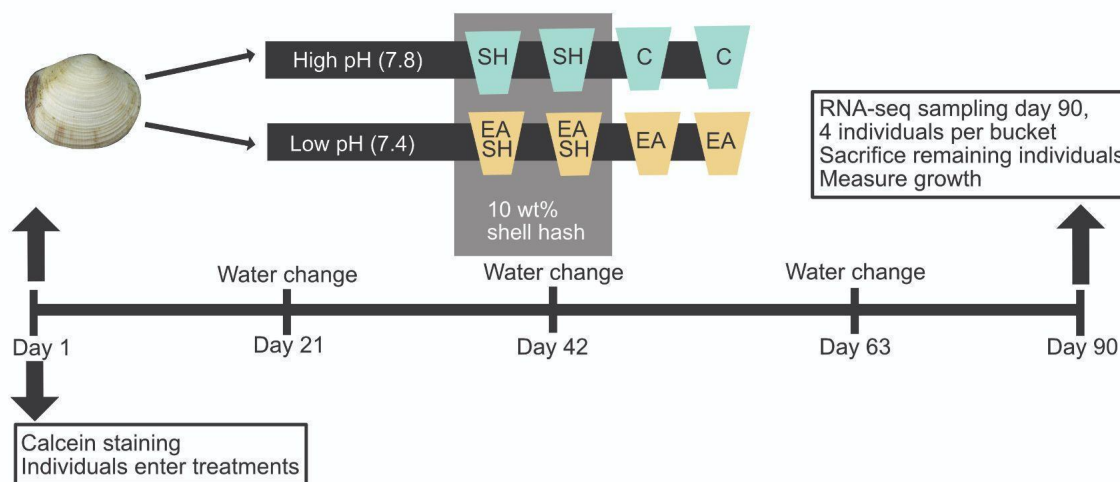
132 Juvenile clams were raised in four experimental conditions for 90 days where the pH of the overlying fluids was maintained
133 in the following ways: (1) control filtered seawater (pH= ~7.8), (2) experimentally acidified seawater (pH= ~7.4), (3) control
134 seawater with shell hash (pH= ~7.8), and (4) acidified seawater with shell hash (pH= ~7.4) (**Fig. 1**). Treatments were run in
135 duplicate, totalling eight ~22.7 L food-grade plastic buckets. Buckets were fed with filtered seawater held in header tanks kept
136 at the ambient temperature of the wet lab space (~15°C), in which pH conditions were controlled using Pinpoint® pH
137 controllers and regulators and a cylinder of compressed air with 1% CO₂ (Airgas) (**Fig. 1**). Probes were briefly removed every
138 Monday and Friday in order to recalibrate using Pinpoint® recalibration fluids (pH = 4.0 and 10.0, NIST scale). Probe
139 measurements were not used to calculate carbonate chemistry parameters, but to maintain approximate target pH conditions
140 for the experiments. Each header tank was supplied with air via an airstone.

141
142 The buckets were filled with filtered seawater for three days prior to the start of the experiment. Buckets were then filled with
143 5 L of unconsolidated medium-grained quartz sand (AquaQuartz; porosity of 38.8%) prior to adding seawater. This silica-
144 based sand was chosen because it has comparable grain size to Bodega Bay sediment, and to minimize confounding variables
145 that could significantly influence carbonate chemistry of the pore fluids via geochemical reactions (e.g., precipitation and
146 dissolution) and/or microbial processes. Disarticulated clam shells were gathered in Bodega Bay, CA, bleached in 6 vol%
147 NaOCl for 30 min to minimize the effects of microorganisms, rinsed thoroughly with fresh water, and air dried for 48 hours.
148 Shells were then crushed using a mortar and pestle, and shell hash pieces were size-graded to 0.25-0.5 cm. All treatments with
149 shell hash contained quartz sand with 10 wt% pulverized shells of *L. staminea* and *Saxidomus nuttalli*, species native to Bodega
150 Bay. The addition of *S. nuttalli* shells, rather than just *L. staminea*, were used to ensure enough aragonitic shell material was
151 available for the experimental setup. Juvenile clams (n=30 per bucket) were placed in each bucket at the beginning of the
152 experiment. Eight liters of cultured *N. oculata* was added every Monday and Friday to the header tanks to feed the animals.
153 Seawater was replaced in the header tanks approximately every three weeks (days 21, 42, 63, and 80). At the end of 90 days,
154 four individuals were sampled from each bucket for genetic analyses, and the remaining living individuals were collected for
155 growth analyses.



156

157



158

159 **Figure 1. Design of 90-day experiment.** SH = shell hash, C = control, EASH = experimental acidification with shell hash,
 160 EA = experimental acidification.

161 **2.3 Calcein staining and fluorescence**

162 All individuals were fluorescently stained with calcein immediately before the experiment to mark the animals' shell length at
 163 the start of the experiment. Following the protocols of Moran and Marko (2005), calcein powder and DI water were combined
 164 to make a concentrated stock solution of 6.25g/L calcein, and the pH of the stock was adjusted to ~7.5 using sodium bicarbonate
 165 to increase the solubility of the calcein. The stock was added to 1L of filtered seawater (final concentration of 100 mg/L)
 166 (Moran & Marko, 2005). After spending 24 hours in this solution, clams were transported to the experimental buckets, and the
 167 90-day experiment began.

168 **2.4 Seawater chemistry**

169 Throughout the duration of the 90-day experiment, seawater in the buckets was sampled for salinity, temperature, pH, and
 170 dissolved oxygen every Monday, Wednesday, and Friday using a Pinpoint® pH probe, a Pinpoint® dissolved oxygen probe,
 171 a thermometer, and a VeeGee refractometer for salinity. Pore water in each bucket was sampled for carbonate chemistry once
 172 per week. Pore water samples were taken using pore water wells (MHE products) from 8 cm depth in the substrate. Pore water



173 was sampled less frequently than overlying fluids to allow the pore fluids more time to interact with shell hash before removing
174 them for sampling.

175

176 Water samples for total pH and total alkalinity were collected for pore water and overlying water in 125 mL glass bottles with
177 a positive meniscus once per week during the mornings (between 7:00 and 10:00 am) to characterize water chemistry. All pH
178 samples were poisoned with mercuric chloride to stop microbial respiration and stored at 4°C or analysed immediately. pH
179 samples were run in duplicate on an Ocean Optics Jaz Spectrophotometer EL200 (SD +/- 0.003) using m-cresol purple dye
180 (Dickson et al., 2007). A calibration regression was produced for m-cresol and calibrated against Tris for a <0.1 pH offset. At
181 the same time, total alkalinity (TA) samples were collected in 125 mL Nalgene with a small amount of headspace, frozen at -
182 20°C, and later analysed by Gran titration using an automatic titrator (809 Titrand, Metrohm) in triplicate. Drift due to changes
183 in temperature was measured with drift catchers every twelve samples. Outliers were removed, and measurements were
184 corrected against Dickson certified reference material (Batch #s 189 and 197). The average precision of the certified reference
185 materials was +/- 3.11 µmol/kg. For runs 4, 5, 6, and 8, where certified reference materials were not analyzed due to instrument
186 malfunctions, samples were secondarily calibrated to known drift catcher values, for which the average precision was +/- 9.2
187 µmol/kg. Alkalinity data from one run (run 9) was discarded due to poor accuracy and precision. Uncertainty of these
188 measurements was included in our statistical analyses. Salinity, pH and alkalinity, and temperature were used to calculate
189 aragonite saturation state (Ω_{Ar}) using the “seacarb” package in R (vers. 4.1.3). Constants for K1 and K2 according to Leuker
190 (2000) and total boron according to Lee et al. (2010) were used.

191

192 **2.5 RNA extraction and quality control protocol**

193 Total RNA was extracted from clam mantle tissue on day 90 of the experiment. Four biological replicates (i.e., four individuals)
194 were chosen from each of the eight buckets at day 90 (n = 32). Total RNA was extracted from the mantle tissue using a TRIzol
195 protocol. Approximately 50-100 mg of mantle tissue was removed from the mantle edge of each clam (i.e., the ridge of tissue
196 near the ventral margin of the shell) using a surgical scalpel equipped with a new blade for each animal. Extractions were
197 performed at ambient room temperature (~19°C) in a fume hood to avoid contamination. 1 mL of TRIzol was added to each
198 tissue sample within five minutes of collection, and the sample was homogenized using an electric pestle. Next, 200 µl
199 chloroform was added and the samples were centrifuged for 15 minutes as 12,000 × g and 4°C to separate the molecular phases.
200 The top aqueous layer was transferred to a new sample tube, and an equal volume of isopropyl alcohol and 1 µl GlycoBlue
201 (ThermoFisher cat #AM9516) was added. After centrifuging the samples again for 10 minutes at 12,000 × g and 4°C, the
202 resulting RNA precipitate was washed with 75% ethanol and air dried before being dissolved in RNase free water.

203

204 Concentration and quality of the RNA extractions were first evaluated using a NanoDrop spectrophotometer and QuBit
205 fluorometer. Once assessed, samples were sent to the UC Davis DNA Technologies and Expression Analysis Core Laboratory,



206 where the raw RNA was then run on an Agilent BioAnalyzer 2100. The highest quality samples (i.e., those with BioAnalyzer
207 RNA integrity numbers > 7) were used for cDNA library prep and sequenced using Illumina High Throughput Sequencing
208 ($n=24$ total, three per bucket). Samples were run on a NovaSeq 6000 S4 flow cell to produce ~ 25 million 150 base pair paired-
209 end reads per sample for all 24 individuals. The quality of raw sequencing data was evaluated using fastQC to identify whether
210 adapter sequences were present (FastQC, 2015). Because adapters were present, we then used Trimmomatic to trim the first
211 15 base pairs from each read to remove adapters (Bolger et al., 2014). These reads are available through the National Center
212 for Biotechnology Information (NCBI), accession PRJNA1011264.

213 **2.6 Mantle transcriptome assembly**

214 As there is no published reference genome for *L. staminea*, we assembled de novo (i.e., reference-free) transcriptomes with
215 the raw Illumina reads in Trinity (Grabherr et al., 2011). The amount of data produced made it computationally infeasible to
216 create a reference transcriptome from all data simultaneously. We therefore created two transcriptomes, each using half of the
217 data, and combined the two datasets using Corset (Davidson & Oshlack, 2014). We mapped the reads back to the transcriptome
218 using Salmon (Patro et al., 2015), with ~ 75 - 82% of reads mapping per dataset.

219
220 The transcriptome was then functionally annotated using Trinotate (Bryant et al., 2017), a comprehensive annotation suite
221 designed for de novo transcriptomes, including a sequence similarity search (Uniprot/SwissProt), protein domain identification
222 (HMMER and PFAM), and eggNog mapper (Cantalapiedra et al., 2021). We also used the Blast2Go program (OmicsBox
223 3.1.9) to get an additional set of annotation predictions for our differentially expressed transcripts by comparing our sequences
224 against the non-redundant protein sequences database on NCBI.

225 **2.7 Differential gene expression analysis**

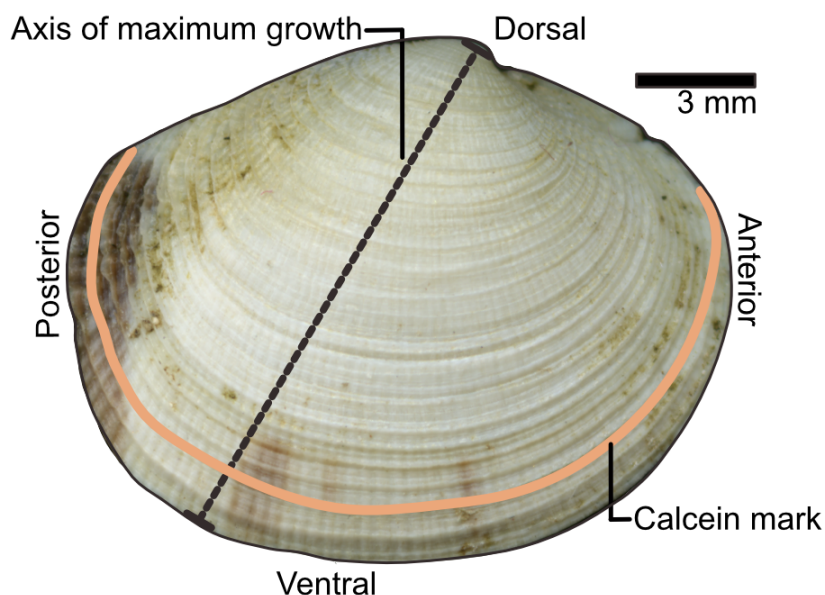
226 To determine which genes were differentially expressed across replicates and treatments, we used the R package edgeR
227 (Robinson et al., 2010) which is part of the Trinity pipeline. Pairwise comparisons of gene expression were performed for all
228 genes in all samples, and correlation heatmaps were produced to compare overall gene expression profile similarity across
229 biological replicates. Genes were considered “differentially expressed” if there was a logarithm of fold change ($\log_{2}FC$) $> |2|$
230 (i.e., a four-fold change in gene expression between experimental conditions) and a false-discovery rate adjusted p-value $<$
231 0.001 . Differentially expressed genes were also annotated using the program Blast2Go (OmicsBox 3.1.9), which searches the
232 National Center for Biotechnology Information (NCBI) protein database using a translated nucleotide sequence, and identified
233 the top 100 protein hits for each of our differentially expressed transcripts.



234 2.8 Shell morphology and growth

235 On day 90, all surviving juvenile clams (n=137) were collected. Soft tissues were removed, immediately frozen at -20 °C and
236 later freeze-dried. Shells were gently cleaned with fresh water and air-dried. We measured the following traits of clam shells:
237 (1) total axis of maximum growth (AMG), (2) new growth along the AMG from the calcein mark, (3) shell dry weight and (4)
238 freeze-dried soft tissue weight (**Fig. 2**). Furthermore, in order to account for differences in shell sizes and growth rates, we
239 calculated the percentage of AMG represented by new growth during the experiment as (5) % new growth = [(new growth
240 (mm) / total axis maximum growth (mm))*100]. Shell weight and soft tissue dry weight were then measured using a Mettler
241 Toledo ME104E scale (0.0001 g). Shell length and AMG were measured using digital calipers (0.001 mm). New growth along
242 the AMG was measured in Fiji (formerly ImageJ) using images taken on a Nikon AZ100 fluorescent microscope (Schindelin
243 et al., 2012) (Supplemental Figure 1).

244



245

246 **Figure 2. Diagram illustrating the measurements taken on *Leukoma staminea* shells.** Image taken on the right valve of a
247 juvenile clam used in this study.

248 2.9 Statistical analyses

249 Two-way analysis of variance (ANOVA) tests were performed to evaluate the statistical relationships between shell growth,
250 carbonate chemistry, and treatment types. Here, two-way ANOVAs tested whether the overlying water pH and/or shell hash
251 affected the pore water pH, pore water alkalinity, and pore water Ω_{Ar} . For morphological characteristics, we tested whether
252 overlying water pH (independent variable 1) and shell hash (independent variable 2) affected the percent of new growth and



253 shell weight (dependent variables). When data were not normally distributed, we transformed them using a log function. For
254 all comparisons, we first ran three ANOVAs: (1) an additive two-way ANOVA (without any interaction or blocking variable),
255 (2) a two-way ANOVA with interaction (sediment type and pH level) but with no blocking variable (bucket ID), and (3) a
256 two-way ANOVA with interaction (sediment type and pH level) and a blocking variable (bucket ID). We then calculated
257 Akaike information criterion (AIC) to determine which ANOVA model best fit the data and reported F-statistics and p-values
258 from that model. As two-way ANOVAs only describe which parameters (i.e., sediment type and overlying pH) are significant,
259 post-hoc Tukey Honestly-Significant-Different (HSD) tests were conducted to test for pairwise differences between groups
260 (C, SH, EA, EASH). Lastly, to investigate bucket effects on growth, a linear mixed effects model was applied using restricted
261 maximum likelihood in the lme4 package in R. The model predicted the percent new growth with treatment as a fixed-effect
262 parameter and bucket ID as a nested random-effect within treatment. The call for this model in lme4 was: `percent_new_growth`
263 `~ treatment + (1 | bucket.id/treatment)`. All statistical tests were performed in R (version 3.5.3).

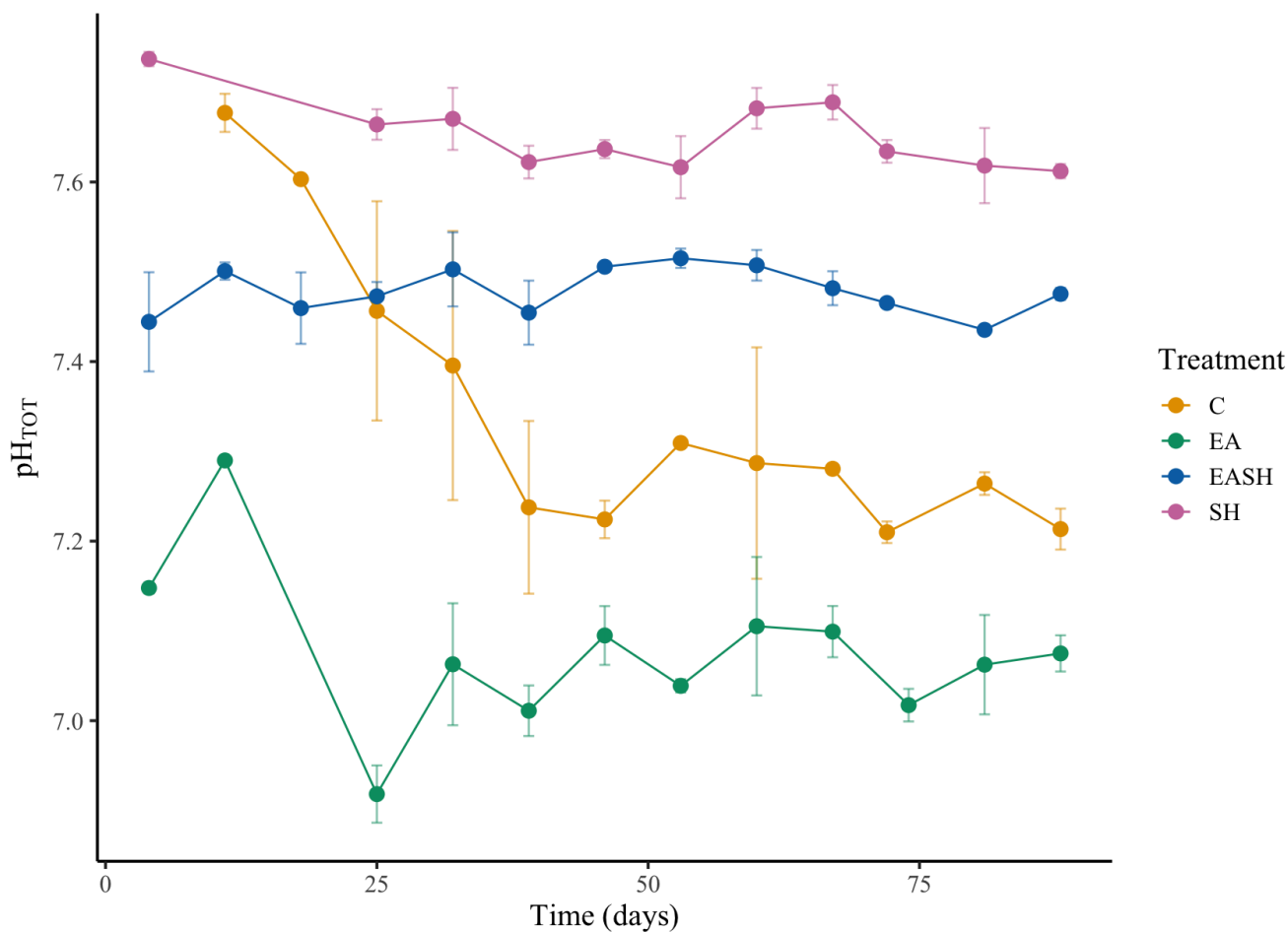
264 **3 Results**

265 **3.1 Terminology**

266 For readability, we will use the following terms for our experimental conditions: “C” = control (seawater pH ~7.8, no shell
267 hash in the sediment); “SH” = shell hash (seawater pH ~7.8; shell hash added); “EA” = experimental acidification (seawater
268 pH ~7.4, no shell hash in the sediment); “EASH” = experimental acidification plus shell hash (seawater pH ~7.4, no shell hash
269 in the sediment).

270 **3.2 Seawater chemistry**

271 Salinity, temperature, and dissolved oxygen remained relatively constant over the course of the 90-day experiment (**Table 1**;
272 **SI Table 1**). All pH values of the overlying water demonstrate the experimental design was successful in maintaining the
273 desired values around 7.4 and 7.8. The pH of the pore water was generally stable through the course of the experiment (**Figure**
274 **3**) although there was a notable drop in pore water pH in the control condition over time. pH values did not vary significantly
275 among technical replicates (T-test: $p > 0.05$), and we therefore pooled replicate data for calculating means and standard
276 deviations (**SI Table 1**).



277

278 **Figure 3. Porewater pH_{TOT} over time (days).** Points on the plot show the mean values, and error bars denote one standard
 279 deviation. A set of samples from the beginning of the experiment are missing due to sampling error.

280

281 **Table 1.** Means and standard deviations for salinity, temperature, dissolved oxygen, and pH measured in the header tanks
 282 (acidified and control) over the course of the 90-day experiment.

Header tank	Salinity (ppt)	Temperature (°C)	Dissolved Oxygen (mg/L)	pH (in situ)
Acidified	34.6 +/- 0.500	15.7 +/- 0.490	8.22 +/- 0.569	7.80 +/- 0.039
Control	34.6 +/- 0.510	15.7 +/- 0.490	8.25 +/- 0.471	7.31 +/- 0.028

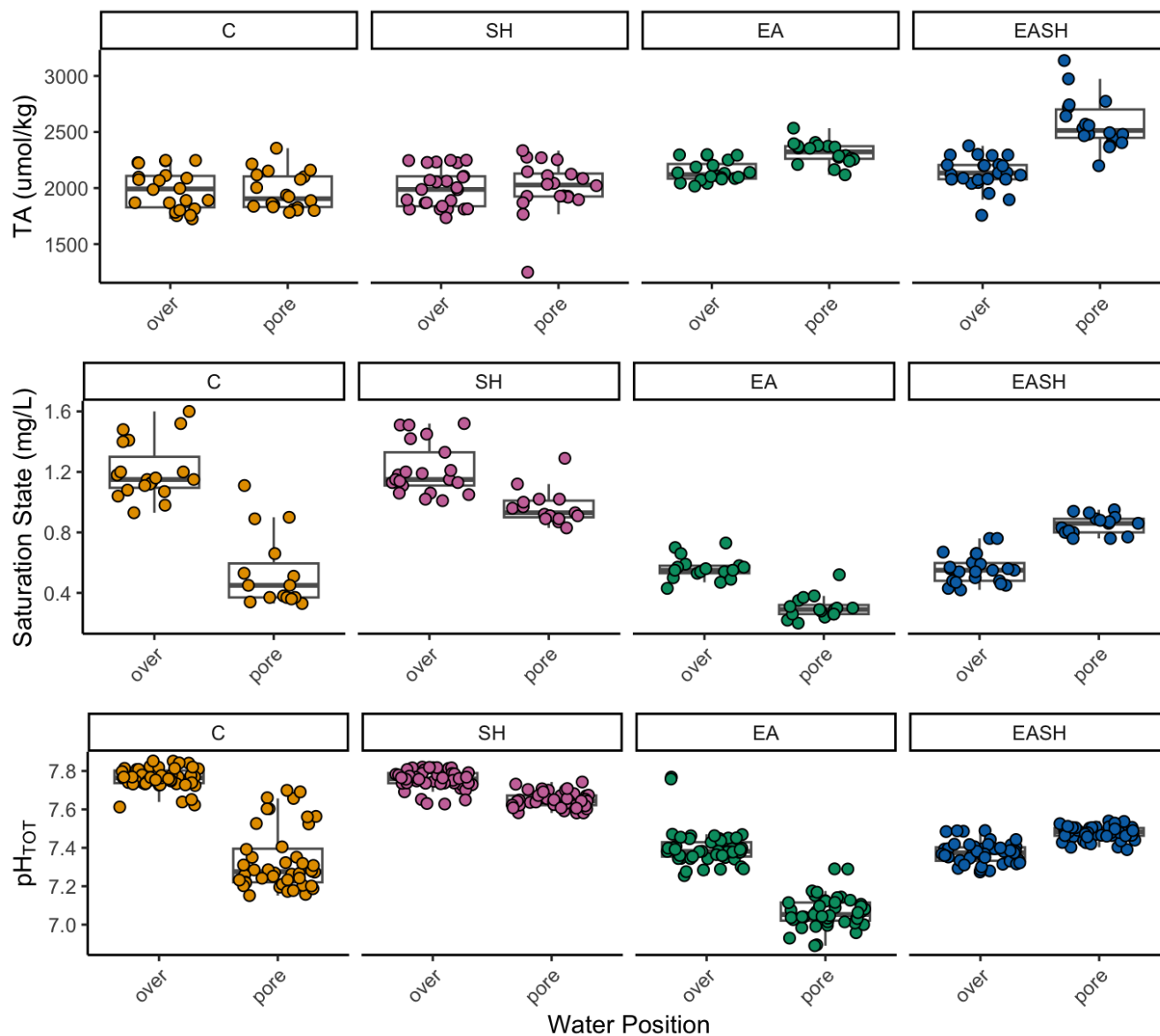
283

284 The different treatments show markedly different seawater chemistry. Box plots of the data are provided in **Fig. 4** and are
 285 consistent with expectations. In the control, pore water pH and Ω_{Ar} values are markedly lower than the overlying seawater.
 286 Adding shell hash raises these values in the pore water, while experimentally acidifying the overlying water lowers these



287 values in the pore waters. Adding shell hash to experimentally acidified treatments increases pH and Ω_{Ar} values in the pore
288 water, with Ω_{Ar} values comparable to what is seen in the non-acidified treatment. Using two-way ANOVA tests, we confirmed
289 that the sediment type (shell hash vs. no shell hash) and overlying pH (acidified or non-acidified) had a significant effect on
290 pore water alkalinity, pH and Ω_{Ar} (**Table 2**) and Tukey post-hoc tests for all carbonate chemistry parameters revealed
291 significant pairwise differences between many treatments based on presence/absence of shell hash and overlying pH (**Table**
292 **3**). In summary, pore water pH decreased when the overlying seawater had a low pH, but that was countered by the addition
293 of shell hash to the sediment.

294



295

296

297

298

299

300

301

Figure 4 Box plots depicting total alkalinity (TA), aragonite saturation state, and pH_{TOT} for all treatments. Results are separated between pore water and overlying water measurements. C = control; SH = shell hash; EA = experimental acidification; EASH = experimental acidification + shell hash.



	Df	Sum Sq	Mean Sq	F value	Pr(>F)
Alkalinity					
sed_type	1	0.0473	0.0473	5.050	0.0281
over_pH	1	0.7360	0.7360	78.625	9.66e-13
sed_type:over_pH	1	0.0462	0.0462	4.931	0.0299
Residuals	64	0.5991	0.0094		
pH					
sed_type	1	0.07884	0.07884	196.999	< 2e-16
over_pH	1	0.02975	0.02975	74.339	3.83e-15
sed_type:over_pH	1	0.00172	0.00172	4.298	0.0396
Residuals	175	0.07004	0.0004		
Saturation State (Ω_{Ar})					
sed_type	1	8.465	8.465	112.44	2.78e-14
over_pH	1	1.751	1.751	23.25	1.42e-05
sed_type:over_pH	1	0.707	0.707	9.39	0.00354
Residuals	49	3.689	0.075		

302

303

Table 2. ANOVA tests for water alkalinity, pH and Ω_{Ar} . Interaction models are reported here; see the associated code for results from all ANOVA model tests. Key: “sed_type” = sediment type (shell hash vs. no shell hash); “over_pH” = overlying seawater pH (normal vs. experimentally acidified seawater).

304

305

306

Tukey HSD Results for Pore Water Chemistry ($p < 0.001$)		
pH	Alkalinity	Saturation State
SH:C EA:C EASH:C EA:SH EASH:SH SH:EA	SH:C EA:C EASH:C EA:SH EASH:SH EASH:EA	SH:C EA:C EASH:C EA:SH EASH:EA

307



308 **Table 3.** Tukey post-hoc tests for all pore water carbonate chemistry parameters analyzed with two-way ANOVA. Significant
 309 pairwise differences between treatments based on presence/absence of shell hash (sand vs. sand with shell hash) and overlying
 310 pH (low vs. high) are shown for pH, alkalinity and aragonite saturation state.

311
 312 **3.3 Shell morphology and growth**

313 At the end of 90 days, 137 clams survived. Calcein stains were reliably produced in most individuals, with only a small subset
 314 lacking distinct lines (n=7). Therefore, a total of 130 clams were measured and compared statistically at the end of the
 315 experiment. Average percent new growth varied markedly across treatments (**Table 4**), with those in shell hash (SH) treatment
 316 growing the most (9.38 +/- 7.24 % new growth) and those in the experimental acidification (EA) treatment growing the least
 317 (5.65 +/- 3.50 % new growth). Two-way ANOVAs revealed that differences in average percent new growth were statistically
 318 significant due to overlying pH [F(1)=5.82, p = 0.0173], but not presence/absence of shell hash [F(1)=3.01, p = 0.085], and
 319 the interaction between these metrics was not statistically significant (p = 0.066). However, Tukey HSD post-hoc tests for
 320 percent new growth suggest the EA treatment had significantly lower growth when compared to the other treatments. Two-
 321 way ANOVAs and Tukey HSDs did not identify statistically significant differences in shell weight or tissue weight across
 322 treatments with overlying pH or sediment type (p > 0.05). Bucket effects did not affect growth metrics, with only 0.154%
 323 variance explained by bucket ID (SI Table 2). Our results suggest that, despite high variation in growth across treatments,
 324 animals experiencing experimental acidification and shell hash had a higher rate of shell growth than those experiencing
 325 experimental acidification only, and that these animals were statistically indistinguishable from the control.

326

	Shell length (mm)	Total AMG (mm)	Growth on AMG (mm)	% New growth	Shell weight (g)	Tissue dry weight (mg)
C	12.4 +/- 4.21	11.5 +/- 3.76	1.05 +/- 0.815	8.30 +/- 4.24	0.604 +/- 0.485	47.5 +/- 39.7
SH	13.2 +/- 4.33	11.1 +/- 3.45	1.13 +/- 0.963	9.38 +/- 7.24	0.611 +/- 0.538	49.7 +/- 44.3
EA	12.8 +/- 3.53	10.7 +/- 2.91	0.670 +/- 0.510	5.65 +/- 3.50	0.468 +/- 0.374	35.7 +/- 27.9
EASH	12.8 +/- 3.97	11.0 +/- 3.15	0.873 +/- .500	7.46 +/- 3.35	0.486 +/- 0.414	37.5 +/- 31.5

327

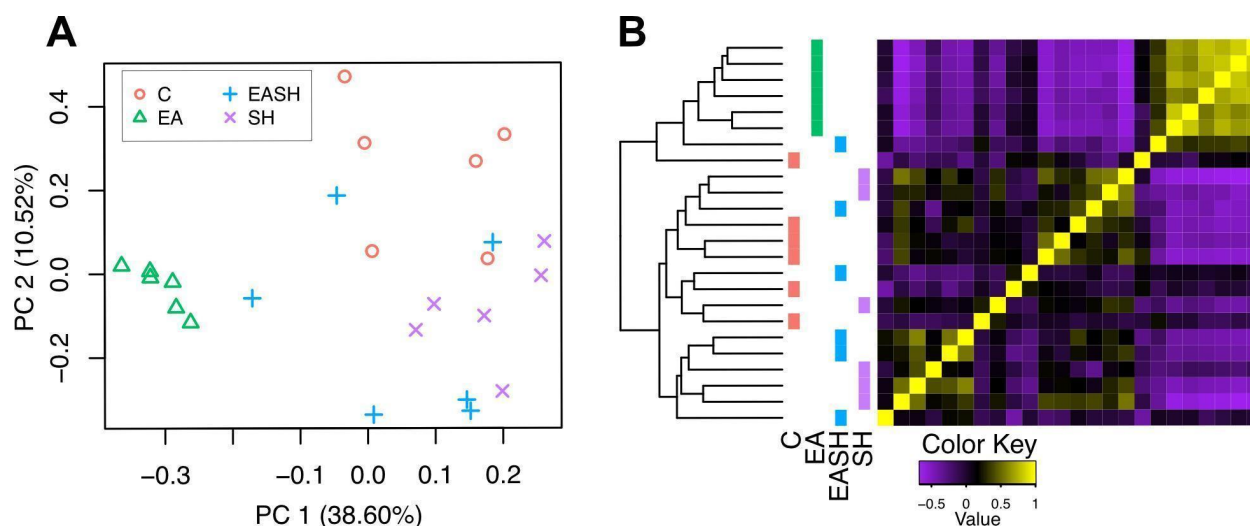
328 **Table 4. Morphological metrics measured on day 90.** Averages and standard deviations are shown. AMG = axis of
 329 maximum growth, C = normal pH conditions, SH= normal conditions with shell hash, EA = experimental acidification, EASH
 330 = experimental acidification + shell hash.



331

332 3.4 Gene Expression Analysis

333 Our transcriptome of *L. staminea* mantle tissue included 638,598 transcript models, which clustered into 530,958 gene models.
 334 This number is likely far higher than the actual number of genes present, but this is not unusual for a *de novo* transcriptome
 335 assembly (Haas et al., 2013; Raghavan et al., 2022). 284 genes were found to be differentially expressed, based on a cutoff of
 336 a p-value < 0.001 and a > 4-fold change in expression between two or more conditions. Notably, the experimentally acidified
 337 (EA) treatment looked markedly different from all other treatments. The principal components plot (Fig. 5A) and sample
 338 correlation matrix (Fig. 5B) demonstrate that the replicates from the EA treatment cluster together, while the other conditions
 339 are intermixed. These plots are consistent with the numbers of differentially expressed genes recovered; excluding the EA
 340 condition, no more than 11 of the 284 genes were differentially expressed in any pairwise comparisons. This suggests that the
 341 addition of shell hash to experimentally acidified water resulted in a gene expression profile largely indistinguishable from
 342 animals raised in non-acidified conditions, with or without shell hash.



343

344 **Figure 5. Overview of differential gene expression analysis.** (A) PCA plot demonstrating similarity among the replicates,
 345 based on the count of differentially expressed genes. (B) A correlation matrix of the same data, with the count data log
 346 transformed and centered around the mean. Note how, in both analyses, the EA replicates cluster together, while samples from
 347 all other conditions are intermixed.

348

349 While the broad pattern of gene expression supports our hypothesis that adding shell hash would result in a loss of pH-stress
 350 genetic signatures, we were only able to annotate a small subsample of the genes, which limited our ability to understand the
 351 range of biological processes being impacted in our experiment. The vast majority of our 284 differentially expressed genes
 352 failed to receive an annotation in the Trinotate pipeline; a second approach using BLAST2GO did only marginally better (see
 353 **SI Table 3** for details). Attempts to identify enriched biological pathways based on gene annotations failed to recover any



354 statistically significant results. We therefore performed several additional analyses to look for possible genes that play a role
355 in response to ocean acidification.

356

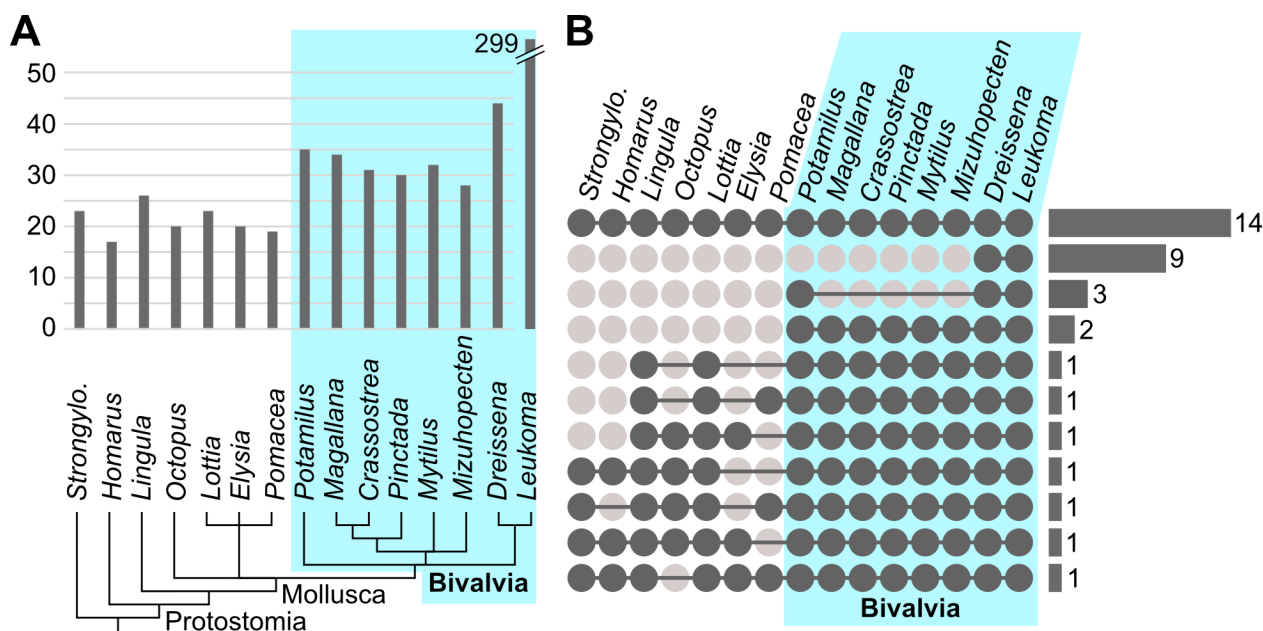
357 Firstly, we tested if any differentially expressed genes were shared between two or more treatments, looking for genes generally
358 involved in tolerance to acidified seawater. Twelve genes were differentially expressed in two or more pairwise comparisons.
359 Of these, 10 genes were found in multiple pairwise comparisons against the “EA” condition, suggesting these genes play a
360 general role in acidification tolerance. Unfortunately, only one of these genes was annotated in our pipeline, showing ~79%
361 similarity to “DNA repair protein complementing XPA cells homolog” of the Manila clam *Ruditapes philippinarum*. In mice,
362 the XPA protein plays a critical role in nucleotide excision repair in response to ultraviolet and chemical damage (de Vries &
363 van Steeg, 1996; Pan & Lee, 2009); it is unclear whether the *L. staminea* gene plays a similar role, but we note that four
364 additional differentially expressed genes were similarly annotated as XPA-like proteins, and the role of XPA proteins in *L.*
365 *staminea* in response to ocean acidification is worth exploring further.

366

367 We also tested how many of our differentially expressed genes could be identified in other bivalves, with the thought that these
368 genes, though potentially unannotated, could reveal important clade-specific regulators of acidification tolerance. We
369 downloaded a reference proteome for every bivalve genus in the UniProt database (<https://www.uniprot.org/>), as well as a
370 selection of non-bivalve animal outgroups. We then used BLASTx to compare our differentially expressed *L. staminea*
371 transcripts against these proteomes, using an e-value cutoff of 10e-10. The results of this analysis are shown in **Fig. 6** (and
372 detailed in SI Table 4). We tested 299 transcripts predicted from the 284 gene models (Trinity attempts to predict isoforms, so
373 there are often more transcripts than gene models), yet only 49 matched to a sequence in one or more proteomes. There is some
374 phylogenetic signal in the data, with the highest number of matches coming from *Dreissena polymorpha*—which, like *L.*
375 *staminea*, is part of the taxonomic superorder Imparidentia—and bivalves generally showed a larger number of matches than
376 other animals (Figure 6A). Fourteen transcripts were found across all datasets. Most of these appear to be general cell
377 maintenance genes, but one notable exception is a perlucin-like protein, which is known to regulate calcium carbonate
378 precipitation in some molluscs and is necessary for proper shell growth in oysters raised in acidified seawater (Schwaner et
379 al., 2023). We also identified a putative monocarboxylate transporter, which has been recovered in other experimental
380 acidification studies on bivalves, and is hypothesized to transport ions to the site of biomineralization (Li et al., 2022; Sleight
381 et al., 2020). Another two transcripts from *L. staminea* matched sequences present in all analyzed bivalve proteomes. Both had
382 annotations, including a putative NADPH oxidase 5-like gene, which has also been identified in Atlantic surf clams (*Spisula*
383 *solidissima*) exposed to acute heat stress (Acquafredda et al., 2024). A final nine sequences were uniquely shared between *D.*
384 *polymorpha* and *L. staminea*; most of these were unannotated and we found no evidence that the few genes with annotations
385 had been identified in previous bivalve RNA-Seq studies. These results do not support the hypothesis that our dataset is



386 enriched in bivalve-specific genes, but this exercise did reveal some important genes thought to regulate environmental
 387 tolerance and/or biomineralization in other species.



388
 389 **Figure 6. Summary of sequence similarity between the differentially expressed genes in this study and proteomes from**
 390 **other species.** (A) A plot showing the number of matching sequences between *L.staminea* and other genera, with a
 391 phylogenetic tree at the bottom showing evolutionary relationships. (B) An UpSet plot visualizing the shared number of
 392 transcripts found in *L.staminea* and other organisms. All other combinations resulted in one or fewer shared genes. In both
 393 images, the bivalves are highlighted in blue; “Strongylo.” = *Strongylocentrotus*.

394 **4 Discussion**

395 Our results suggest that shell hash can lessen the effects of acidification by buffering the chemistry of pore fluids, thus
 396 providing a potential acidification mitigation strategy for infaunal organisms like clams (Curtin et al., 2022; Doyle & Bendell,
 397 2022; Ericson & Ragg, 2021; Green et al., 2013; Salter, 2018). Gene expression profiling of clam mantle tissue suggested that
 398 shell hash was beneficial for the clams, as the “acidification” signal present in animals grown under low-pH conditions
 399 disappeared when shell hash was added. Further, despite high variability in growth metrics across individuals—which
 400 complicated our statistical analyses—our results suggest the addition of shell hash to experimentally acidified water resulted
 401 in greater *L. staminea* shell growth, to the point that it was statistically indistinguishable from the control population. In the
 402 future, additional studies using animals of the same size—alongside age and genetic cohort—may help disentangle individual
 403 variability from the effects of acidification on shell growth.



404

405 Additional research should investigate shell hash buffering in natural settings. Existing studies on the role of shell hash in
406 moderating pore water chemistry have had variable results, and local environmental conditions appear critically important
407 (Beal et al., 2020; Curtin et al., 2022; Doyle & Bendell, 2022; Green et al., 2009, 2013; Greiner et al., 2018). Still, our research
408 provides clear support for the hypothesis that shell hash can buffer pore water chemistry, and mitigates a natural tendency for
409 pore water pH to decrease over time (Figure 3). Therefore, this study warrants continued research investigating scalability,
410 efficacy, and safety of using shell hash to buffer acidification. Further research is also needed to assess the ability of shell hash
411 to buffer acidic conditions at the water-sediment interface where larvae first settle and clams' siphons extend (Green et al.,
412 2009; Waldbusser et al., 2015). This research is needed for many infaunal species, as compounding environmental stressors
413 could yield conditions that are too corrosive for larval settlement and development (Doyle & Bendell, 2022; Green et al., 2009;
414 Waldbusser et al., 2015).

415

416 **5 Conclusions**

417 In conclusion, this experimental study suggests that shell hash buffers acidic conditions in pore waters and benefits clam
418 growth. Implementation of this technique in coastal settings, however, would best be considered on a site-by-site basis, and
419 include partnerships with Indigenous communities and other experts with an understanding of local practices. The controlled
420 conditions of the laboratory ignore variables that will likely dictate the success of field projects, such as the chemical and
421 microbial complexity of natural sediments and tidal influences. Finally, our findings further point towards the need for research
422 and stewardship explored in collaboration with Indigenous communities who continue to visit, gather from, and care for
423 intertidal spaces. This study, like all research, is conducted on Indigenous land, and “place always matters” (Justice 2016, 21).
424 As documented elsewhere on the Pacific Coast (Groesbeck et al., 2014; Lepofsky et al., 2015), tending coastal Californian
425 clam beds is grounded in Indigenous systems of knowledge. We draw from current calls to braid Indigenous science with
426 western science, and other “boundary spanning” approaches, that support the goals and interests of Indigenous communities,
427 not science alone (Whyte et al. 2016; Atalay, 2020; Hatch et al., 2023; Kimmerer & Artelle, 2024 White et al., 2024; Wickham
428 et al., 2022). In all, this experiment provides significant evidence of shell hash buffering capacity, and provides promising
429 results to prompt future collaborative research in coastal settings on clam bed tending in the face of continued climate change.

430

431

432 **Data Availability**

433 The genetic data produced in this study is accessible on NCBI (Accession: PRJNA1011264). The code used to analyze the
434 data is provided on GitHub at https://github.com/DavidGoldLab/2025_Leukoma_RNA-Seq (Zenodo DOI
435 [10.5281/zenodo.19488331](https://doi.org/10.5281/zenodo.19488331)). Shell images are available on Harvard Dataverse at <https://doi.org/10.7910/DVN/DL8BY0>.

436



437

438 **Author contributions**

439

440 HLK: conceptualization, investigation, model experiments, funding acquisition, formal analysis, visualization, and writing
441 (original draft preparation). AJG: methodology and writing (review and editing). TMH: methodology and writing (review and
442 editing). TDS: supervision, conceptualization, and writing (review and editing). SJC: project administration, supervision,
443 conceptualization, and writing (review and editing). DAG: project administration, supervision, conceptualization, formal
444 analysis, funding acquisition and writing (original draft preparation).

445

446 **Competing interests**

447 The contact author has declared that none of the authors has any competing interests.

448

449 **Financial support**

450 This work was supported by California Sea Grant (project Number: R/HCE-22F awarded to H.L.K. and D.A.G) and a Russell
451 J. and Dorothy S. Bilinski Fellowship to H.L.K.

452

453 **7 Supplemental Figure Legends**

454

455 Supplemental Figure 1. Example fluorescent image of a calcein-stained shell. Area of the shell within the blue lines indicates
456 shell growth during the duration of the experiment. Red line indicates the length of new growth. All shell images are available
457 on Harvard Dataverse at <https://doi.org/10.7910/DVN/DL8BY0>.

458

459

460 Supplemental Figure 2. pH measurements from Pinpoint® probes in the overlying water plotted over time for all buckets.
461 Dotted lines show average for acidified and non-acidified treatments.

462

463 **8 Supplemental Table Legends**

464

465 Supplemental Table 1. Mean values and standard deviations for pH and aragonite saturation state (Ω) of overlying water and
466 pore waters in the bucket treatments. Sample results here were taken once weekly for spectrophotometric pH analysis and
467 alkalinity titrations. OA = acidification, OASH = acidification + shell hash, C = control, and SH= control pH with shell hash.

468



469 Supplemental Table 2. Summary of linear mixed effects model fit to percent new shell for clams at the end of the 90-day
470 experimental period. Fixed effects (i.e., treatment) have constant, systematic influence on the dependent variable (here, percent
471 new shell). Random effects (i.e., bucket replicate ID) account for random variability not directly related to independent
472 variables.

473

474 Supplemental Table 3. Annotation of differentially expressed genes in the *L. staminea* transcriptome. Full data can be found
475 on GitHub, file “DE_Genes_Summary.xlsx”.

476

477 Supplemental Table 4. Results of BLASTp analyses comparing the differentially expressed *L. staminea* protein models with
478 proteomes from select animals. Full results can be found on GitHub in folder “7_DE_Genes”.

479

480 **9 Supplemental Data**

481

482 Supplemental Sheet 1. Complete list of cleaned total pH data.

483

484 Supplemental Sheet 2. Complete list of cleaned total alkalinity data.

485

486 Supplemental Sheet 3. Complete calculated carbonate system data using the R package ‘seacarb’.

487

488 Supplemental Sheet 4. Complete list of pH measurements using Pinpoint® probes.

489

490 Supplemental Sheet 5. Complete list of salinity measurements using VeeGee refractometer.

491

492 Supplemental Sheet 6. Complete list of dissolved oxygen measurements using Pinpoint® probes.

493

494 Supplemental Sheet 7. Complete list of temperature measurements using a digital thermometer.

495

496 Supplemental Sheet 8. Table with raw clam growth data measured day 90 of the experiment.

497 **References**

498 Miller, B. B. and Carter, C.: The test article, *J. Sci. Res.*, 12, 135–147, doi:10.1234/56789, 2015.

499 Smith, A. A., Carter, C., and Miller, B. B.: More test articles, *J. Adv. Res.*, 35, 13–28, doi:10.2345/67890, 2014.



- 500
501
502
503 Acquafredda, M., Guo, X., and Munroe, D. (2024). Transcriptomic Response of the Atlantic Surfclam (*Spisula solidissima*)
504 to Acute Heat Stress. *Marine Biotechnology*, 26(1), 149–168. <https://doi.org/10.1007/s10126-024-10285-0>
- 505 Aller, R. C. (1982). The Effects of Macrobenthos on Chemical Properties of Marine Sediment and Overlying Water. In P. L.
506 McCall & M. J. S. Tevesz (Eds.), *Animal-Sediment Relations: The Biogenic Alteration of Sediments* (pp. 53–102). Springer
507 US. https://doi.org/10.1007/978-1-4757-1317-6_2
- 508 Andersson, A. J., & Mackenzie, F. T. (2011). Effects of Ocean Acidification on Benthic Processes, Organisms, and
509 Ecosystems. In J.-P. Gattuso & L. Hansson (Eds.), *Ocean Acidification* (p. 0). Oxford University Press.
510 <https://doi.org/10.1093/oso/9780199591091.003.0012>
- 511 Atalay, S. (2020). Indigenous Science for a World in Crisis. *Public Archaeology*, 19(1–4), 37–52.
512 <https://doi.org/10.1080/14655187.2020.1781492>
- 513 Barber, J. S., Ruff, C. P., McArdle, J. T., Hunter, L. L., Speck, C. A., Rogers, D. W., & Greiner, C. M. (2019). Intertidal clams
514 exhibit population synchrony across spatial and temporal scales. *Limnology and Oceanography*, 64(S1), S284–S300.
515 <https://doi.org/10.1002/lno.11085>
- 516 Barton, A., Waldbusser, G., Feely, R., Weisberg, S., Newton, J., Hales, B., Cudd, S., Eudeline, B., Langdon, C., Jefferds, I.,
517 King, T., Suhrbier, A., & McLaughlin, K. (2015). Impacts of Coastal Acidification on the Pacific Northwest Shellfish Industry
518 and Adaptation Strategies Implemented in Response. *Oceanography*, 25, 146–159. <https://doi.org/10.5670/oceanog.2015.38>
- 519 Beal, B. F., Coffin, C. R., Randall, S. F., Goodenow, C. A., Pepperman, K. E., & Ellis, B. W. (2020). Interactive effects of
520 shell hash and predator exclusion on 0-year class recruits of two infaunal intertidal bivalve species in Maine, USA. *Journal of*
521 *Experimental Marine Biology and Ecology*, 530–531, 151441. <https://doi.org/10.1016/j.jembe.2020.151441>
- 522 Bednaršek, N., Feely, R. A., Howes, E. L., Hunt, B. P. V., Kessouri, F., León, P., Lischka, S., Maas, A. E., McLaughlin, K.,
523 Nezlin, N. P., Sutula, M., and Weisberg, S. B.: Systematic review and meta-analysis toward synthesis of thresholds of ocean
524 acidification impacts on calcifying pteropods and interactions with warming, *Front. Mar. Sci.*, 6, 227,
525 <https://doi.org/10.3389/fmars.2019.00227>, 2019.
- 526 Bendell, L. I. (2014). Evidence for Declines in the Native *Leukoma staminea* as a Result of the Intentional Introduction of the
527 Non-native *Venerupis philippinarum* in Coastal British Columbia, Canada. *Estuaries and Coasts*, 12.
- 528 Bolger, A. M., Lohse, M., & Usadel, B. (2014). Trimmomatic: A flexible trimmer for Illumina sequence data. *Bioinformatics*,
529 30(15), 2114–2120. <https://doi.org/10.1093/bioinformatics/btu170>
- 530 Bryant, D. M., Johnson, K., DiTommaso, T., Tickle, T., Couger, M. B., Payzin-Dogru, D., Lee, T. J., Leigh, N. D., Kuo, T.-
531 H., Davis, F. G., Bateman, J., Bryant, S., Guzikowski, A. R., Tsai, S. L., Coyne, S., Ye, W. W., Freeman, R. M., Peshkin, L.,



- 532 Tabin, C. J., ... Whited, J. L. (2017). A Tissue-Mapped Axolotl De Novo Transcriptome Enables Identification of Limb
533 Regeneration Factors. *Cell Reports*, 18(3), 762–776. <https://doi.org/10.1016/j.celrep.2016.12.063>
- 534 Burdige, D. J., Zimmerman, R. C., & Hu, X. (2008). Rates of carbonate dissolution in permeable sediments estimated from
535 pore-water profiles: The role of sea grasses. *Limnology and Oceanography*, 53(2), 549–565.
536 <https://doi.org/10.4319/lo.2008.53.2.0549>
- 537 Caldeira, K., Wickett, M. Anthropogenic carbon and ocean pH. *Nature* 425, 365 (2003).
538 <https://doi.org/10.1038/425365a>
- 539 Caldeira, K., & Wickett, M. E. (2005). Ocean model predictions of chemistry changes from carbon dioxide emissions to the
540 atmosphere and ocean. *Journal of Geophysical Research: Oceans*, 110(C9). <https://doi.org/10.1029/2004JC002671>
- 541 Cantalapiedra, C. P., Hernández-Plaza, A., Letunic, I., Bork, P., & Huerta-Cepas, J. (2021). eggNOG-mapper v2: Functional
542 Annotation, Orthology Assignments, and Domain Prediction at the Metagenomic Scale. *Molecular Biology and Evolution*,
543 38(12), 5825–5829. <https://doi.org/10.1093/molbev/msab293>
- 544 Checkley, D., & Barth, J. (2009). Patterns and processes in the California Current System. *Progress In Oceanography*, 83, 49–
545 64. <https://doi.org/10.1016/j.pocean.2009.07.028>
- 546 Clements, J. C., & Chopin, T. (2017). Ocean acidification and marine aquaculture in North America: Potential impacts and
547 mitigation strategies. *Reviews in Aquaculture*, 9(4), 326–341. <https://doi.org/10.1111/raq.12140>
- 548 Cox, K. D., Gerwing, T. G., Macdonald, T., Hessian-Lewis, M., Millard-Martin, B., Command, R. J., Juanes, F., & Dudas, S.
549 E. (2019). Infaunal community responses to ancient clam gardens. *ICES Journal of Marine Science*, 76(7), 2362–2373.
550 <https://doi.org/10.1093/icesjms/fsz153>
- 551 Cummings, V., Hewitt, J., Van Rooyen, A., Currie, K., Beard, S., Thrush, S., Norkko, J., Barr, N., Heath, P., Halliday, N. J.,
552 Sedcole, R., Gomez, A., McGraw, C., & Metcalf, V. (2011). Ocean Acidification at High Latitudes: Potential Effects on
553 Functioning of the Antarctic Bivalve *Laternula elliptica*. *PLOS ONE*, 6(1), e16069.
554 <https://doi.org/10.1371/journal.pone.0016069>
- 555 Curtin, T. P., Volkenborn, N., Dwyer, I. P., Aller, R. C., Zhu, Q., & Gobler, C. J. (2022). Buffering muds with bivalve shell
556 significantly increases the settlement, growth, survival, and burrowing of the early life stages of the Northern quahog,
557 *Mercenaria mercenaria*, and other calcifying invertebrates. *Estuarine, Coastal and Shelf Science*, 264, 107686.
558 <https://doi.org/10.1016/j.ecss.2021.107686>
- 559 Cusack, M., & Freer, A. (2008). Biomineralization: Elemental and Organic Influence in Carbonate Systems. *Chemical*
560 *Reviews*, 108(11), 4433–4454. <https://doi.org/10.1021/cr078270o>
- 561 Dashfield, S. L., Somerfield, P. J., Widdicombe, S., Austen, M. C., & Nimmo, M. (2008). Impacts of ocean acidification and
562 burrowing urchins on within-sediment pH profiles and subtidal nematode communities. *Journal of Experimental Marine*
563 *Biology and Ecology*, 365(1), 46–52. <https://doi.org/10.1016/j.jembe.2008.07.039>



- 564 Davidson, N. M., & Oshlack, A. (2014). Corset: Enabling differential gene expression analysis for de novo assembled
565 transcriptomes. *Genome Biology*, 15(7), 410. <https://doi.org/10.1186/s13059-014-0410-6>
- 566 Davis, C. V., Hewett, K., Hill, T. M., Largier, J. L., Gaylord, B., & Jahncke, J. (2018). Reconstructing Aragonite Saturation
567 State Based on an Empirical Relationship for Northern California. *Estuaries and Coasts*, 41(7), 2056–2069.
568 <https://doi.org/10.1007/s12237-018-0372-0>
- 569 de Vries, A., & van Steeg, H. (1996). Xpaknockout mice. *Seminars in Cancer Biology*, 7(5), 229–240.
570 <https://doi.org/10.1006/scbi.1996.0031>
- 571 Deur, D., Dick, A., Recalma-Clutesi, K., & Turner, N. J. (2015). Kwakwaka’wakw “Clam Gardens.” *Human Ecology*, 43(2),
572 201–212. <https://doi.org/10.1007/s10745-015-9743-3>
- 573 Dodd, L. F., Grabowski, J. H., Piehler, M. F., Westfield, I., & Ries, J. B. (2021). Juvenile Eastern Oysters More Resilient to
574 Extreme Ocean Acidification than Their Mud Crab Predators. *Geochemistry, Geophysics, Geosystems*, 22(2),
575 e2020GC009180. <https://doi.org/10.1029/2020GC009180>
- 576 Doney, S. C., Busch, D. S., Cooley, S. R., & Kroeker, K. J. (2020). The Impacts of Ocean Acidification on Marine Ecosystems
577 and Reliant Human Communities. *Annual Review of Environment and Resources*, 45(1), 83–112.
578 <https://doi.org/10.1146/annurev-environ-012320-083019>
- 579 Doney, S. C., Fabry, V. J., Feely, R. A., & Kleypas, J. A. (2009). Ocean Acidification: The Other CO₂ Problem. *Annual*
580 *Review of Marine Science*, 1(1), 169–192. <https://doi.org/10.1146/annurev.marine.010908.163834>
- 581 Doyle, B., & Bendell, L. I. (2022). An evaluation of the efficacy of shell hash for the mitigation of intertidal sediment
582 acidification. *Ecosphere*, 13(3), e4003. <https://doi.org/10.1002/ecs2.4003>
- 583 Ericson, J. A., & Ragg, N. L. C. (2021). Effects of crushed mussel, *Perna canaliculus*, shell enrichment on seawater carbonate
584 buffering and development of conspecific larvae exposed to near-future ocean acidification. *Journal of the World Aquaculture*
585 *Society*, n/a(n/a). <https://doi.org/10.1111/jwas.12779>
- 586 FastQC. (2015, June). <https://qubeshub.org/resources/fastqc>
- 587 Feder, H. M., Hendee, J. C., Holmes, P., Mueller, G. J., & Paul, A. J. (1979). Examination of a reproductive cycle of *Protothaca*
588 *staminea* using histology, wet weight-dry weight ratios, and condition indices. *Veliger*, 22(2), 182–187.
- 589 Feely, R. A., Klinger, T., Newton, J. A., & Chadsey, M. (2012). Scientific summary of ocean acidification in Washington State
590 marine waters.
- 591 Feely, R. A., Sabine, C. L., Hernandez-Ayon, J. M., Ianson, D., & Hales, B. (2008). Evidence for Upwelling of Corrosive
592 “Acidified” Water onto the Continental Shelf. *Science*, 320(5882), 1490–1492. <https://doi.org/10.1126/science.1155676>
- 593 Fraser, C. M., & Smith, G. M. (1928). Notes on the ecology of the little neck clam. *Paphia staminea* Conrad. *Trans. R. Soc.*
594 *Can. Ser.*, 3, 249–269.
- 595 Gazeau, F., Quiblier, C., Jansen, J. M., Gattuso, J.-P., Middelburg, J. J., & Heip, C. H. R. (2007). Impact of elevated CO₂ on
596 shellfish calcification. *Geophysical Research Letters*, 34(7). <https://doi.org/10.1029/2006GL028554>



- 597 Gold, D. A., & Vermeij, G. J. (2023). Deep resilience: An evolutionary perspective on calcification in an age of ocean
598 acidification. *Frontiers in Physiology*, 14. <https://www.frontiersin.org/articles/10.3389/fphys.2023.1092321>
- 599 Grabherr, M., Haas, B., Yassour, M. *et al.* Full-length transcriptome assembly from RNA-Seq data without a reference genome.
600 *Nat Biotechnol* 29, 644–652 (2011). <https://doi.org/10.1038/nbt.1883>
- 601 Justice, Daniel Heath 2016 “A Better World Becoming: Placing Critical Indigenous Studies.” In *Critical Indigenous Studies:
602 Engagements in First World Location*, ed. by Aileen Moreton-Robinson, pp. 19–32. Tucson: University of Arizona Press.
- 603 Kleypas, J. A., Buddemeier, R. W., Archer, D., Gattuso, J. P., Langdon, C., & Opdyke, B. N. (1999). Geochemical
604 consequences of increased atmospheric carbon dioxide on coral reefs. *Science (New York, N.Y.)*, 284(5411), 118–120.
605 <https://doi.org/10.1126/science.284.5411.118>
- 606 Lindblad-Toh, K., ... Regev, A. (2011). Full-length transcriptome assembly from RNA-Seq data without a reference genome.
607 *Nature Biotechnology*, 29(7), 644–652. PubMed. <https://doi.org/10.1038/nbt.1883>
- 608 Green, M. A., Jones, M. E., Boudreau, C. L., Moore, R. L., & Westman, B. A. (2004). Dissolution mortality of juvenile
609 bivalves in coastal marine deposits. *Limnology and Oceanography*, 49(3), 727–734. <https://doi.org/10.4319/lo.2004.49.3.0727>
- 610 Green, M. A., Waldbusser, G. G., Hubazc, L., Cathcart, E., & Hall, J. (2013). Carbonate Mineral Saturation State as the
611 Recruitment Cue for Settling Bivalves in Marine Muds. *Estuaries and Coasts*, 36(1), 18–27. <https://doi.org/10.1007/s12237-012-9549-0>
- 612
- 613 Green, M. A., Waldbusser, G. G., Reilly, S. L., Emerson, K., & O’Donnell, S. (2009). Death by dissolution: Sediment
614 saturation state as a mortality factor for juvenile bivalves. *Limnology and Oceanography*, 54(4), 1037–1047.
615 <https://doi.org/10.4319/lo.2009.54.4.1037>
- 616 Greiner, C. M., Klinger, T., Ruesink, J. L., Barber, J. S., & Horwith, M. (2018). Habitat effects of macrophytes and shell on
617 carbonate chemistry and juvenile clam recruitment, survival, and growth. *Journal of Experimental Marine Biology and
618 Ecology*, 509, 8–15. <https://doi.org/10.1016/j.jembe.2018.08.006>
- 619 Groesbeck, A., Rowell, K., Lepofsky, D., & Solomon, A. (2014). Ancient Clam Gardens Increased Shellfish Production:
620 Adaptive Strategies from the Past Can Inform Food Security Today. *PLoS One*, 9(3).
- 621 Haas, B. J., Papanicolaou, A., Yassour, M., Grabherr, M., Blood, P. D., Bowden, J., Couger, M. B., Eccles, D., Li, B., Lieber,
622 M., MacManes, M. D., Ott, M., Orvis, J., Pochet, N., Strozzi, F., Weeks, N., Westerman, R., William, T., Dewey, C. N., ...
623 Regev, A. (2013). De novo transcript sequence reconstruction from RNA-seq using the Trinity platform for reference
624 generation and analysis. *Nature Protocols*, 8(8), 1494–1512. <https://doi.org/10.1038/nprot.2013.084>
- 625 Hatch, M. B. A., Parrish, J. K., Heppell, S. S., Augustine, S., Campbell, L., Divine, L. M., Donatuto, J., Groesbeck, A. S., &
626 Smith, N. F. (2023). Boundary spanners: A critical role for enduring collaborations between Indigenous communities and
627 mainstream scientists. *Ecology and Society*, 28(1). <https://doi.org/10.5751/ES-13887-280141>
- 628 Hickey, B. M., & Banas, N. S. (2003). Oceanography of the U.S. Pacific Northwest Coastal Ocean and estuaries with
629 application to coastal ecology. *Estuaries*, 26(4), 1010–1031. <https://doi.org/10.1007/BF02803360>



- 630 Hiebert, T. C. (2015). *Leukoma staminea*. In *Oregon Estuarine Invertebrates: Rudys' Illustrated Guide to Common Species*
631 (3rd ed.). University of Oregon Libraries and Oregon Institute of Marine Biology.
632 https://scholarsbank.uoregon.edu/xmlui/bitstream/handle/1794/12918/L_staminea_2016_final.pdf?sequence=3
- 633 Hönisch, B., Ridgwell, A., Schmidt, D. N., Thomas, E., Gibbs, S. J., Sluijs, A., Zeebe, R., Kump, L., Martindale, R. C., Greene,
634 S. E., Kiessling, W., Ries, J., Zachos, J. C., Royer, D. L., Barker, S., Marchitto, T. M., Moyer, R., Pelejero, C., Ziveri, P., ...
635 Williams, B. (2012). The Geological Record of Ocean Acidification. *Science*, 335(6072), 1058–1063.
636 <https://doi.org/10.1126/science.1208277>
- 637 Jackley, J., Gardner, L., Djunaedi, A., & Salomon, A. (2016). Ancient clam gardens, traditional management portfolios, and
638 the resilience of coupled human-ocean systems. *Ecology and Society*, 21(4). <https://doi.org/10.5751/ES-08747-210420>
- 639 Kempf, H. L., Gold, D. A., & Carlson, S. J. (2023). Investigating the Relationship between Growth Rate, Shell Morphology,
640 and Trace Element Composition of the Pacific Littleneck Clam (*Leukoma staminea*): Implications for Paleoclimate
641 Reconstructions. *Minerals*, 13(6), Article 6. <https://doi.org/10.3390/min13060814>
- 642 Kimmerer, R. W., & Artelle, K. A. (2024). Time to support Indigenous science. *Science*, 383(6680), 243–243.
643 <https://doi.org/10.1126/science.ado0684>
- 644 Kindeberg, T., Bates, N. R., Courtney, T. A., Cyronak, T., Griffin, A., Mackenzie, F. T., Paulsen, M.-L., & Andersson, A. J.
645 (2020). Porewater Carbonate Chemistry Dynamics in a Temperate and a Subtropical Seagrass System. *Aquatic Geochemistry*,
646 26(4), 375–399. <https://doi.org/10.1007/s10498-020-09378-8>
- 647 Largier, J. L. (2020). Upwelling Bays: How Coastal Upwelling Controls Circulation, Habitat, and Productivity in Bays. *Annual*
648 *Review of Marine Science*, 12(1), 415–447. <https://doi.org/10.1146/annurev-marine-010419-011020>
- 649 Lepofsky, D., Smith, N., Cardinal, N., Harper, J., Morris, M., Elroy White, G., Bouchard, R., Kennedy, D., Solomon, A.,
650 Puckett, M., & Rowell, K. (2015). Ancient Shellfish Mariculture on the Northwest Coast of North America. *American*
651 *Antiquity*, 80(2), 236–259.
- 652 Li, J., Zhou, Y., Qin, Y., Wei, J., Shigong, P., Ma, H., Li, Y., Yuan, X., Zhao, L., Yan, H., Zhang, Y., & Yu, Z. (2022).
653 Assessment of the juvenile vulnerability of symbiont-bearing giant clams to ocean acidification. *Science of The Total*
654 *Environment*, 812, 152265. <https://doi.org/10.1016/j.scitotenv.2021.152265>
- 655 Mackenzie, C. L., Pearce, C. M., Leduc, S., Roth, D., Kellogg, C. T. E., Clemente-Carvalho, R. B. G., & Green, T. J. (2022).
656 Impacts of Seawater pH Buffering on the Larval Microbiome and Carry-Over Effects on Later-Life Disease Susceptibility in
657 Pacific Oysters. *Applied and Environmental Microbiology*, 88(22), e0165422. <https://doi.org/10.1128/aem.01654-22>
- 658 Mackenzie, F. T., & Andersson, A. J. (2011). Biological Control on Diagenesis: Influence of Bacteria and Relevance to Ocean
659 Acidification. In J. Reitner & V. Thiel (Eds.), *Encyclopedia of Geobiology* (pp. 137–143). Springer Netherlands.
660 https://doi.org/10.1007/978-1-4020-9212-1_73
- 661 Macreadie, P. I., Anton, A., Raven, J. A., Beaumont, N., Connolly, R. M., Friess, D. A., Kelleway, J. J., Kennedy, H., Kuwae,
662 T., Lavery, P. S., Lovelock, C. E., Smale, D. A., Apostolaki, E. T., Atwood, T. B., Baldock, J., Bianchi, T. S., Chmura, G. L.,



- 663 Eyre, B. D., Fourqurean, J. W., ... Duarte, C. M. (2019). The future of Blue Carbon science. *Nature Communications*, 10,
664 3998. <https://doi.org/10.1038/s41467-019-11693-w>
- 665 Middelburg, J. J., Soetaert, K., & Hagens, M. (2020). Ocean Alkalinity, Buffering and Biogeochemical Processes. *Reviews of*
666 *Geophysics*, 58(3), e2019RG000681. <https://doi.org/10.1029/2019RG000681>
- 667 Moran, A., & Marko, P. (2005). A Simple Technique for Physical Marking of Larvae of Marine Bivalves. *Journal of Shellfish*
668 *Research*, 24(2), 567–571. [https://doi.org/10.2983/0730-8000\(2005\)24\[567:ASTFPM\]2.0.CO;2](https://doi.org/10.2983/0730-8000(2005)24[567:ASTFPM]2.0.CO;2)
- 669 Orr, J. C., Fabry, V. J., Aumont, O., Bopp, L., Doney, S. C., Feely, R. A., Gnanadesikan, A., Gruber, N., Ishida, A., Joos, F.,
670 Key, R. M., Lindsay, K., Maier-Reimer, E., Matear, R., Monfray, P., Mouchet, A., Najjar, R. G., Plattner, G.-K., Rodgers, K.
671 B., ... Yool, A. (2005). Anthropogenic ocean acidification over the twenty-first century and its impact on calcifying organisms.
672 *Nature*, 437(7059), Article 7059. <https://doi.org/10.1038/nature04095>
- 673 Pan, Y.-R., & Lee, E. Y.-H. P. (2009). UV-dependent interaction between Cep164 and XPA mediates localization of Cep164
674 at sites of DNA damage and UV sensitivity. *Cell Cycle*, 8(4), 655–664. <https://doi.org/10.4161/cc.8.4.7844>
- 675 Patro, R., Duggal, G., & Kingsford, C. (2015). Salmon: Accurate, Versatile and Ultrafast Quantification from RNA-seq Data
676 using Lightweight-Alignment. *bioRxiv*, 021592. <https://doi.org/10.1101/021592>
- 677 Raghavan, V., Kraft, L., Mesny, F., & Rigerte, L. (2022). A simple guide to de novo transcriptome assembly and annotation.
678 *Briefings in Bioinformatics*, 23(2), bbab563. <https://doi.org/10.1093/bib/bbab563>
- 679 Renforth, P., & Henderson, G. (2017). Assessing ocean alkalinity for carbon sequestration. *Reviews of Geophysics*, 55(3),
680 636–674. <https://doi.org/10.1002/2016RG000533>
- 681 Ries, J. B., Cohen, A. L., & McCorkle, D. C. (2009). Marine calcifiers exhibit mixed responses to CO₂-induced ocean
682 acidification. *Geology*, 37(12), 1131–1134. <https://doi.org/10.1130/G30210A.1>
- 683 Robinson, M. D., McCarthy, D. J., & Smyth, G. K. (2010). edgeR: A Bioconductor package for differential expression analysis
684 of digital gene expression data. *Bioinformatics*, 26(1), 139–140. <https://doi.org/10.1093/bioinformatics/btp616>
- 685 Sabine, C. L., Feely, R. A., Gruber, N., Key, R. M., Lee, K., Bullister, J. L., Wanninkhof, R., Wong, C. S., Wallace, D. W. R.,
686 Tilbrook, B., Millero, F. J., Peng, T.-H., Kozyr, A., Ono, T., & Rios, A. F. (2004). The Oceanic Sink for Anthropogenic CO₂.
687 *Science*, 305(5682), 367–371. <https://doi.org/10.1126/science.1097403>
- 688 Saderne, V., Geraldini, N. R., Macreadie, P. I., Maher, D. T., Middelburg, J. J., Serrano, O., Almahasheer, H., Arias-Ortiz, A.,
689 Cusack, M., Eyre, B. D., Fourqurean, J. W., Kennedy, H., Krause-Jensen, D., Kuwae, T., Lavery, P. S., Lovelock, C. E., Marba,
690 N., Masqué, P., Mateo, M. A., ... Duarte, C. M. (2019). Role of carbonate burial in Blue Carbon budgets. *Nature*
691 *Communications*, 10(1), Article 1. <https://doi.org/10.1038/s41467-019-08842-6>
- 692 Salter, N. (2018). Ancient clam gardens magnify bivalve production by moderating ambient temperature and enhancing
693 sediment carbonate. Master of Resource Management Thesis, Simon Fraser University. 79 pps.



- 694 Schindelin, J., Arganda-Carreras, I., Frise, E., Kaynig, V., Longair, M., Pietzsch, T., Preibisch, S., Rueden, C., Saalfeld, S.,
695 Schmid, B., Tinevez, J.-Y., White, D. J., Hartenstein, V., Eliceiri, K., Tomancak, P., & Cardona, A. (2012). Fiji: An open-
696 source platform for biological-image analysis. *Nature Methods*, 9(7), 676–682. <https://doi.org/10.1038/nmeth.2019>
- 697 Schneider, T., DeAntoni, G., Hill, A., & Apodaca, A. (2018). Indigenous Persistence and Foodways at the Toms Point Trading
698 Post (CA-MRN-202), Tomales Bay, California. *Journal of California and Great Basin Anthropology*, 38(1), 51–73.
- 699 Schwaner, C., Pales Espinosa, E., & Allam, B. (2023). RNAi Silencing of the Biomineralization Gene Perlucin Impairs Oyster
700 Ability to Cope with Ocean Acidification. *International Journal of Molecular Sciences*, 24(4).
701 <https://doi.org/10.3390/ijms24043661>
- 702 Sleight, V. A., Antczak, P., Falciani, F., & Clark, M. S. (2020). Computationally
703 predicted gene regulatory networks in molluscan biomineralization identify extracellular matrix production and ion
704 transportation pathways. *Bioinformatics*, 36(5), 1326–1332. <https://doi.org/10.1093/bioinformatics/btz754>
- 705 Tadlock, S. (2019). “One day you’re gonna know you won’t starve here”: Thesis for Masters of Public Health, University of
706 Washington.
- 707 Takesue, R. K., & van Geen, A. (2004). Mg/Ca, Sr/Ca, and stable isotopes in modern and Holocene *Protothaca staminea* shells
708 from a northern California coastal upwelling region. *Geochimica et Cosmochimica Acta*, 68(19), 3845–3861.
<https://doi.org/10.1016/j.gca.2004.03.021>
- 709 Toniello, G., Lepofsky, D., Lertzman-Lepofsky, G., Salomon, A., & Rowell, K. (2019). 11,500 y of human–clam relationships
710 provide long- term context for intertidal management in the Salish Sea, British Columbia. *PNAS*, 116(44), 22106–22114.
- 711 Waldbusser, G. G., Hales, B., Langdon, C. J., Haley, B. A., Schrader, P., Brunner, E. L., Gray, M. W., Miller, C. A., &
712 Gimenez, I. (2015). Saturation-state sensitivity of marine bivalve larvae to ocean acidification. *Nature Climate Change*, 5(3),
713 273–280. <https://doi.org/10.1038/nclimate2479>
- 714 Wallace, R. B., Baumann, H., Grear, J. S., Aller, R. C., & Gobler, C. J. (2014). Coastal ocean acidification: The other
715 eutrophication problem. *Estuarine, Coastal and Shelf Science*, 148, 1–13. <https://doi.org/10.1016/j.ecss.2014.05.027>
- 716 White, Elroy (Q̇íẋitasu), Kyle A. Artelle, Ed Brown (Ḣúmpaṡ ł̇úẋv), Kelly Brown (ł̇áq̇vamut), Diana E. Chan, and
717 William Housty (Ḋúqv̇áiṡla) 2024 Ṁnúẋv̇it model for centering Indigenous knowledge and governance. *Conservation*
718 *Biology* 38:e14398. DOI: 10.1111/cobi.14398.
- 719 Whyte, K.P., Brewer, J.P. & Johnson, J.T. Weaving Indigenous science, protocols and sustainability science. *Sustain Sci* 11,
720 25–32 (2016). <https://doi.org/10.1007/s11625-015-0296-6>
- 721 Wickham, Sara B., Skye Augustine, Andra Forney, Darcy L. Mathews, Nancy Shackelford, Jennifer Walkus, and
722 Andrew J. Trant 2022 Incorporating place-based values into ecological restoration. *Ecology and Society* 27(3):32. DOI:
723 10.5751/ES-13370-270332.
- 724 Widdicombe, S., Spicer, J., & Kitidis, V. (2011). Effects of ocean acidification on sediment fauna. *Ocean Acidification*, 176–
725 191.

<https://doi.org/10.5194/egusphere-2026-1930>

Preprint. Discussion started: 22 April 2026

© Author(s) 2026. CC BY 4.0 License.



- 726 Zachos, J. C., Dickens, G. R., & Zeebe, R. E. (2008). An early Cenozoic perspective on greenhouse warming and carbon-cycle
727 dynamics. *Nature*, 451(7176), Article 7176. <https://doi.org/10.1038/nature06588>
- 728 Zeebe, R. E., & Wolf-Gladrow, D. (2001). *CO₂ in Seawater: Equilibrium, Kinetics, Isotopes*. Gulf Professional Publishing.